JOURNAL OF APPLIED TOXICOLOGY
J. Appl. Toxicol. 2008; **28**: 175–182
Published online 20 June 2007 in Wiley InterScience
(www.interscience.wiley.com) DOI: 10.1002/jat.1263

Zinc toxicity alters mitochondrial metabolism and leads to decreased ATP production in hepatocytes

Joseph Lemire, Ryan Mailloux and Vasu D. Appanna*

Department of Chemistry and Biochemistry, Laurentian University, Sudbury, Ontario P3E 2C6, Canada

Received 9 February 2007; Revised 19 March 2007; Accepted 30 March 2007

ABSTRACT: Although zinc (Zn) is a known environmental toxicant, its impact on the cellular energy-producing machinery is not well established. This study investigated the influence of this divalent metal on the oxidative ATP producing network in human hepatocellular carcinoma (HepG2) cells. Zn-challenged cells contained more oxidized proteins and lipids compared with control cells. Zn severely impeded mitochondrial functions by inhibiting aconitase, α-ketoglutarate dehydrogenase, isocitrate dehydrogenase-NAD$^+$ dependent, succinate dehydrogenase and cytochrome C oxidase Zn-exposed cells had a disparate mitochondrial metabolism compared with the control cells and produced significantly less ATP. However, the expression of isocitrate dehydrogenase-NADP$^+$ dependent was more prominent in cells treated with Zn. Hence, Zn-induced pathologies may be due to the inability of the mitochondria to generate energy effectively.

KEY WORDS: zinc; mitochondrial metabolism; ATP production; aconitase; succinate dehydrogenase; TCA cycle

Introduction

Zinc is an essential trace element due to its participation in a variety of biological processes. Zinc is involved in numerous enzymatic reactions, plays a pivotal role in transcription, cell signaling and in the regulation of cellular pH (Hambidge, 2000). Zinc deficiency is often characterized by compromised T-cell function, neurosensory injury and hindered healing processes (Piao *et al*., 2003; Prasad, 1996; Sandstead, 1991). However, in elevated concentrations, Zn is toxic. It is a significant component of ambient particulate matter (PM) and it is also an important pollutant in industrial settings (Barceloux, 1999; Coleman, 1992). This divalent metal has been implicated in neurological disorders, in the disruption of iron homeostasis, and has also been shown to perturb cholesterol metabolism (Fosmire, 1990; Religa *et al*., 2006). Although there have been numerous studies on Zn toxicity, there is a dearth of information on the influence of this metal on mitochondrial energy production.

In aerobic organisms, the mitochondria are the main supplier of energy and are the site of the tricarboxylic acid (TCA) cycle, a metabolic network involved in the generation of reducing factors that power the production of ATP (Costello *et al*., 1997; Fernie *et al*., 2004; Manev *et al*., 1997). Within this organelle reside numerous enzymes that may be potential targets of Zn. The ability of aluminum (Al) to inhibit the TCA cycle enzymes, to impede ATP synthesis and to promote anaerobiosis via HIF-1α stabilization was recently demonstrated (Mailloux and Appanna, 2007; Mailloux *et al*., 2006a, 2006b). Zn has been shown to promote ROS (Reactive Oxygen Species) via the displacement of bioavailable Fe, the binding of GSH (Glutathione) molecules, and it is known to inhibit some key TCA cycle enzymes (Dinely *et al*., 2003; Gazaryan *et al*., 2002; Koh *et al*., 1996; Sensi *et al*., 1999). However, the exact mechanism(s) of how this divalent metal interferes with oxidative-ATP production is not fully understood. This report describes the ability of Zn to inhibit numerous mitochondrial enzymes and to perturb ATP production in human liver cells. The implication of the diminished activities of aconitase (ACN) and cytochrome C oxidase (Cyt C Ox) on various disease processes, as a consequence of Zn toxicity, is also discussed.

Methods

Cell Culture, Isolation and Fractionation

Human hepatocellular carcinoma (Hep G2) cells were a gift from Dr Templeton (University of Toronto) and were maintained in α-MEM containing 5% FBS and 1% antibiotics. The cells were routinely seeded at 100 000 cells ml^{-1} in 175 cm^2 culture flasks and incubated with 5% CO_2 in a humidified atmosphere operating at 37 °C. Upon reaching 70% confluency the cell monolayer was washed with PBS and the cultures were

* Correspondence to: V. D. Appanna, Department of Chemistry and Biochemistry, Laurentian University, Sudbury, Ontario P3E 2C6, Canada.
E-mail: VAppanna@laurentian.ca
Contract/grant sponsor: Industry Canada.

re-supplemented with serum-free media reconstituted with 2.5 mM citrate (control), 2.5 mM citrate: 50 μM $ZnCl_2$ [note that the normal serum concentration of Zn is 15 μM (Steinebach and Wolterbeek, 1993; Takeda *et al*., 2001; Walsh *et al*., 1994)] or 2.5 mM citrate: 50 μM H_2O_2. These concentrations of Zn and H_2O_2 are known to be toxic (Abordo *et al*., 1999; Canzoniero *et al*., 1999; Dumont *et al*., 1999). Cell viability was monitored with trypan blue exclusion assay (Shannon, 1978). Following the 24 h stress period, the media was removed and the cells were washed with PBS [136.8 mM sodium chloride, 2.5 mM potassium chloride, 1.83 mM dibasic sodium phosphate, and 0.431 mM monobasic potassium phosphate (pH 7.4)]. Cells were harvested by trypsinization and then centrifuged at 250 *g* for 10 min at 4 °C. The cellular pellet was resuspended in cell storage buffer (CSB) (50 mM Tris-HCl, 1 mM phenylmethylsulphonylfluoride, 1 mM dithiothreitol, 250 mM sucrose, 2 mM citrate, containing 1 mg ml^{-1} of pepstatin A and 0.1 mg ml^{-1} of leupeptin) and stored at −86 °C until needed. The cells were thawed and pelleted by centrifugation at 250 *g* for 10 min at 4 °C. The pellet was re-suspended in a minimal volume of CSB (4×10^6 cells/50 μl). The resultant cell suspension was disrupted on ice using a Brunswick sonicator, operating for 5 s with 1 s bursts. Whole cells and nuclei were removed by centrifugation at 850 *g* for 10 min at 4 °C. The mitochondria were then isolated from the cytoplasm via differential centrifugation, 12 000 *g* for 30 min at 4 °C. Following the centrifugation, the soluble fraction (supernatant) was placed in an ice cold eppendorf and the mitochondrial pellet was resuspended in a minimal amount of CSB. Protein quantification was ascertained via the Bradford assay (Bradford, 1976) and BSA was utilized as the standard to normalize the assay.

Oxidized Protein and Lipid Analyses

To evaluate oxidized lipid content in the membrane, the thiobarbituric acid reactive species assay (TBARS) was performed as described in Aydin *et al*. (2005). The fraction containing the membrane portion was solubilized in a mixture containing 15% trichloroacetic acid, 0.375% trichlorobarbituric acid and 0.25 N HCl. The reaction mixture was subsequently heated for 20 min at 100 °C. The precipitated protein was then pelleted at 21 000 *g* for 10 min and the supernatant was monitored at 532 nm. Reaction mixtures lacking trichlorobarbituric acid were used as negative controls.

Protein carbonyl content was determined by performing a dinitrophenyl hydrazine (DNPH) assay as described in Costello *et al*. (1997). One mg of soluble protein was homogenized with 1 ml of 2% (w/v) DNPH and reacted for 1 h. The protein was subsequently precipitated and the pellet was washed thrice with ethylacetate:ethanol (1:1). 1 ml of 6 M guanidine-HCl was added to the mixture and read spectrophotometrically at 360 nm. Reaction mixtures lacking DNPH were used as negative controls.

Blue Native PAGE (BN PAGE) and Protein Activity Assays

BN PAGE was performed according to the method described by Beriault and Schagger (Beriault *et al*., 2007; Schagger and von Jagow, 1991). 4–10% gradient gels were cast in a BioRad MiniProtean™ 2 electrophoresis unit. Samples of 2 μg of protein equivalent μl^{-1} were prepared in blue native buffer (500 mM 6-amino hexanoic acid, 50 mM BisTris (pH 7.0) and 1% β-dodecyl-D-maltoside). β-dodecyl-D-maltoside was omitted in the case of soluble proteins. 30 μg of the prepared protein samples was loaded into each well of the native gel. For migration through the stacking gel, the unit was run at 80 V. For the resolving gel the electrophoresis was run at 200 V. The blue cathode buffer [50 mM Tricine, 15 mM BisTris, 0.02% w/v Coomassie G-250 (pH 7.0) at 4 °C] was exchanged for colourless cathode [50 mM Tricine, 15 mM BisTris (pH 7.0) at 4 °C] once the running front was half way through the resolving gel. Upon completion, the gel slab was removed and incubated in an equilibration buffer (25 mM Tris-HCl, 5 mM $MgCl_2$ (pH 7.4) for 15 min. Enzyme activity was visualized with the aid of formazan precipitation. The gels were incubated in reaction mixture containing equilibration buffer, 5 mM substrate, 0.5 mM cofactor, 0.5 mg ml^{-1} iodonitrotetrazolium chloride (INT) and 0.2 mg ml^{-1} phenazine methosulphate (PMS). Isocitrate dehydrogenase (ICDH) activity was ascertained with 5 mM isocitrate, 0.1 mM NAD^+ or $NADP^+$, PMS and INT. α-Ketoglutarate dehydrogenase (α-KGDH) activity was made apparent with 5 mM α-ketoglutarate, 0.1 mM NAD^+, 0.25 mM CoA, PMS and INT. The concentration of NAD^+ and $NADP^+$ used was 0.1 mM to prevent cross reactivity. Cyt C Ox activity was deduced with the utilization of equilibration buffer supplemented with KCN (5 mM), 10 mg ml^{-1} of diaminobenzidine, 10 mg ml^{-1} cytochrome C and 562.5 mg ml^{-1} of sucrose.

Two dimensional SDS-PAGE was performed on the activity bands as described in (Mailloux *et al*., 2006b). Band specificity was confirmed by using standard enzymes. The purity of mitochondrial and cytoplasmic fractions was confirmed by VDAC (voltage dependent anion channels) and F-Actin immunoblots. Activity bands were subsequently quantified using Scion imaging software for Windows.

Immunoblot Analysis

SDS PAGE and 2D SDS-PAGE gels were performed according to the modified method described by Laemmli

DOI: 10.1002/jat

(1970). Protein samples were first solubilized in 62.5 mM Tris-HCl (pH 6.8), 2% SDS and 2% β-mercaptoethanol at 100 °C for 5 min. The protein samples were then loaded in a 10% isocratic gel and electrophoresed using a discontinuous buffer system. For 2D immunoblot analysis, activity bands from native gels were precision cut from the gel and incubated in denaturing buffer (1% β-mercaptoethanol, 5% SDS) for 30 min, and then placed vertically into the well of the SDS gel. Following completion of the SDS electrophoresis, the proteins were transferred electrophoretically to a Hybond™ — P polyvinylidene difluoride membrane for immunoblotting. Non-specific binding sites were blocked by treating the membrane with 5% non fat skim milk dissolved in TTBS [20 mM Tris-HCl, 0.8% NaCl, 1% Tween-20 (pH 7.6)] for 1 h.

Polyclonal antibodies raised against mitochondrial $NADP^+$-ICDH, ACN and KGDH were generous gifts from Dr S. Yokota, University of Yamanashi, Dr R. Eisenstein, University of Wisconsin-Madison and Dr G. Lindsay, University of Glasgow, respectively. The secondary antibodies (Santa Cruz) consisted of horseradish peroxidase-conjugated mouse anti-rabbit. The detection relied on incubation of the probed membrane for 5 min at room temperature in the presence of Chemiglow reagent (Alpha Innotech). Visualization of the immunoblot was documented via a ChemiDoc XRS system (Biorad Imaging Systems).

Metabolite Analysis

To further ascertain the effect of zinc on the mitochondria, mitochondrial isolate (2 mg ml^{-1} protein equivalent) obtained from control and Zn stressed conditions were incubated in a phosphate buffer [10 mM phosphate, 5 mM $MgCl_2$ (pH 7.4)] containing 1 mM citrate, 0.1 mM NAD^+ and 0.5 mM ADP for 1 h at 37 °C. The reaction was stopped by the addition of ice cold 0.1% perchloric acid. The organic acids and nucleotides were extracted for HPLC analysis (Samizo *et al*., 2001). The resultant spent fluid from the reaction was analysed using a C_{18}-reverse phase column (Phenomenex) with the aid of an Alliance HPLC (Waters). The mobile phase used consisted of 20 mM KH_2PO_4 (pH 2.9 with 6 N HCl), operating at an elution rate of 0.7 ml min^{-1} at ambient temperature. The identities of the metabolites were compared with known standards, or reaction mixtures were spiked with the appropriate standards. The initial levels of metabolites were obtained by running the reaction mixture at time zero.

Fluorescence Microscopy

The impact of Zn on mitochondrial activity was achieved using immunofluorescence. Cells were grown to a minimal density on coverslips and incubated for 24 h in the presence of serum-free α-MEM containing either 2.5 mM cit or 2.5 mM cit: 50 µM $ZnCl_2$. The coverslips were washed once with 0.5 mM EDTA and twice with PBS to ensure all residual zinc was removed. The cells were incubated in 10 µg ml^{-1} Rhodamine B, diluted in α-MEM for 20 min at 37 °C. The cells were then fixed with methanol:acetic acid (3:1). Coverslips were then submerged in a Tween-20 Tris-buffered saline (TTBS) solution with 5% FBS for 1 h to permeabilize the membrane. The coverslip was then washed three times with Tris-buffered saline (TBS). The hepatocytes were then incubated for 2 h in anti-VDAC antibody diluted (1/400) in TBS/5% FBS solution. The coverslips were washed thoroughly and incubated in anti-rabbit FITC conjugate. Following antibody exposure the cells were washed and mounted onto microscope slides. The cells were visualized using an inverted deconvolution microscope (Zeiss). The protonated Rhodamine B molecule was detected at $\lambda_{excitation}$ = 564 nm and $\lambda_{emission}$ = 620 nm. Similarly the fluorescein isothiocyanate was dectected at $\lambda_{excitation}$ = 495 nm and $\lambda_{emission}$ = 520 nm, allowing the distinction of the mitochondria.

Statistical Analysis

All experiments were done three times and in duplicate (where appropriate standard deviations are given). Statistical significance was analysed using Student's *t*-test.

Results and Discussion

In an effort to evaluate the toxic impact of zinc on energy production, HepG2 cells were exposed to zinc for 24 h and mitochondrial functions were assessed. 50 µM Zn has been shown to be associated with Zn toxicity in humans (Steinebach and Wolterbeek, 1993; Walsh *et al*., 1994). A 25% reduction in cell viability was observed. Rhodamine B revealed a diminished proton gradient in HepG2 mitochondria exposed to Zn (Fig. 1). The more intense fluorescence was an indication of an increased proton gradient in the control cells. Rhodamine B is known to provide a visual indication of the activity of the mitochondrion. The interaction between the Rhodamine B and the mitochondrion was further confirmed by the detection of the voltage dependent mitochondrial porin VDAC, an important mitochondrial marker. The spots due to Rhodamine B fluorescence correspond to those of the VDAC (FITC) fluorescence, thus confirming the localization of the mitochondria. This decrease in mitochondrial fluorescence in Zn-challenged cells prompted us to evaluate the oxidative stress triggered by Zn. Indeed, a drastic increase in oxidized lipids and proteins was observed in the Zn-stressed cells (Table 1). This would undoubtedly lead to mitochondrial dysfunction. As

DOI: 10.1002/jat

Table 1. Oxidized lipids and proteins in control and Zn-exposed HepG2 cells

Treatment	Oxidized lipids (μmol[a]/4 × 10^6 cells)	Oxidized protein (pmol[b]/4 × 10^6 cells)
Control	0.050 ± 0.016	0.339 ± 0.096[c]
Zn stressed	0.156 ± 0.093	1.209 ± 0.058[c]

n = 3, mean ± SD.
[a] Malondialdehyde equivalents (μmol).
[b] Carbonyl equivalents (ρmol).
[c] Denotes a statistically significant difference in comparison with control ($P \leq 0.05$).

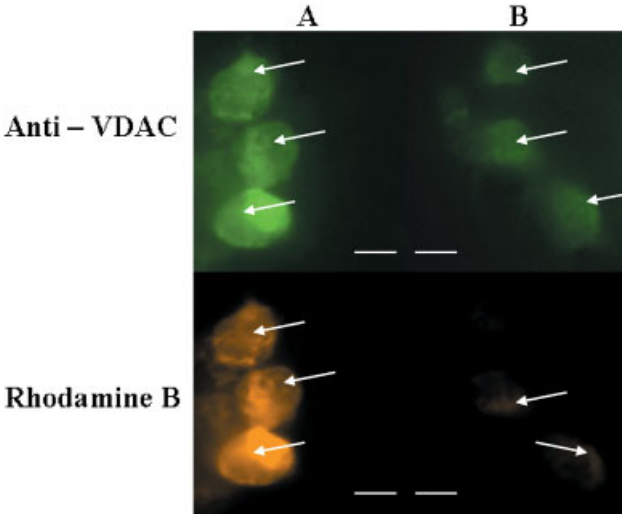

Figure 1. Immunofluorescent detection of mitochondrial activity: HepG2 cells were grown on a glass coverslip until minimal confluency and then exposed to (A) citrate and (B) Zn-citrate for 24 h. The mitochondria were visualized with anti-VDAC and Rhodamine B. Scale bar: 10 μm. This figure is available in colour online at www.interscience.wiley.com/journal/jat

Zn seemed to be interfering with aerobic energy metabolism, the mitochondria's capability to metabolize citrate was assessed. Mitochondria from control and Zn-stressed HepG2 cells that were incubated for 1 h in the presence of citrate and NAD^+ were analysed by HPLC. Higher citrate levels were evident in the Zn-stressed HepG2 mitochondria as opposed to control mitochondria (Fig. 2, I). In addition, higher levels of α-KG were also present in the HepG2 mitochondria challenged with Zn. These chromatographic studies confirmed the inability of the Zn-stressed HepG2 mitochondria to appropriately metabolize citrate. Higher amounts of citrate and α-KG in the Zn-stressed mitochondria indicated that this divalent metal may affect various enzymes contributing to the TCA cycle. Aconitase, an enzyme essential in the isomerization of citrate was evaluated (Fig. 2, II). A marked decrease in the expression of this enzyme was observed in the mitochondria isolated from the Zn-stressed cells. However, similar levels were evident in the cytoplasmic fraction. The purity of these cellular fractions was ascertained with F-actin and VDAC immunoblots (Fig. 2, III and IV). As Zn was triggering oxidative stress, the cells were also exposed to H_2O_2 in order to assess the similarities/differences between these two insults. KGDH is a key enzyme in the TCA cycle involved in the production of NADH, a consequence of the oxidative decarboxylation of α-KG. KGDH activity was ascertained by native PAGE using NAD^+, CoA and α-KG. The KGDH in the Zn-stressed mitochondria displayed lower activity in comparison with the control (Fig. 3, I). A decreased KGDH activity was also observed in cells exposed to H_2O_2. To evaluate the amount of protein associated with the activity stain, the bands were excised and treated for 2D immunoblot analysis. The intensity of the bands did not appear to vary significantly among the three conditions (Fig. 3, II). It is important to note that H_2O_2 and Zn appeared to elicit a similar response in regard to KGDH. As Zn seemed to interfere with the KGDH-mediated production of NADH, other enzymes critical in the aerobic production of NADH were also examined. NAD^+-ICDH activity was severely hampered in HepG2 cells exposed to Zn (Fig. 3, III). In contrast, the activity of this enzyme seemed to be unaffected in the control cells. To assess the influence of Zn on oxidative metabolism further, two key enzymes involved in oxidative phosphorylation, SDH and Cyt C Ox, were probed. In-gel activity staining of SDH pointed to the diminished capacity of this enzyme to metabolize succinate in the Zn-stressed HepG2 cells (Fig. 3, IV). Similarly, the amount of diaminobenzidene precipitated at the site of Cyt C Ox activity was severely impeded in the Zn-stressed HepG2 cells (Fig. 3, V). The inhibition of SDH and Cyt C Ox was also confirmed in cells exposed to H_2O_2. Since NAD^+-ICDH was diminished in the Zn-challenged cells that were characterized by higher amounts of α-KG; it was decided to evaluate the status of $NADP^+$-ICDH, an enzyme that produces α-KG. This enzyme has also been localized in the mitochondria where it has been shown to play a pivotal role in maintaining a reductive environment. Enhanced activity of the cytoplasmic $NADP^+$-ICDH was observed in the cells exposed Zn (Fig. 4, I). Mitochondrial $NADP^+$-ICDH exposed to Zn and H_2O_2 also showed an increase in activity (Fig. 4, II). The activity bands were excised and electrophoresed by the 2D-PAGE technique. Subsequent silver staining and immunoblot analysis revealed more protein associated with the activity band from the cells

DOI: 10.1002/jat

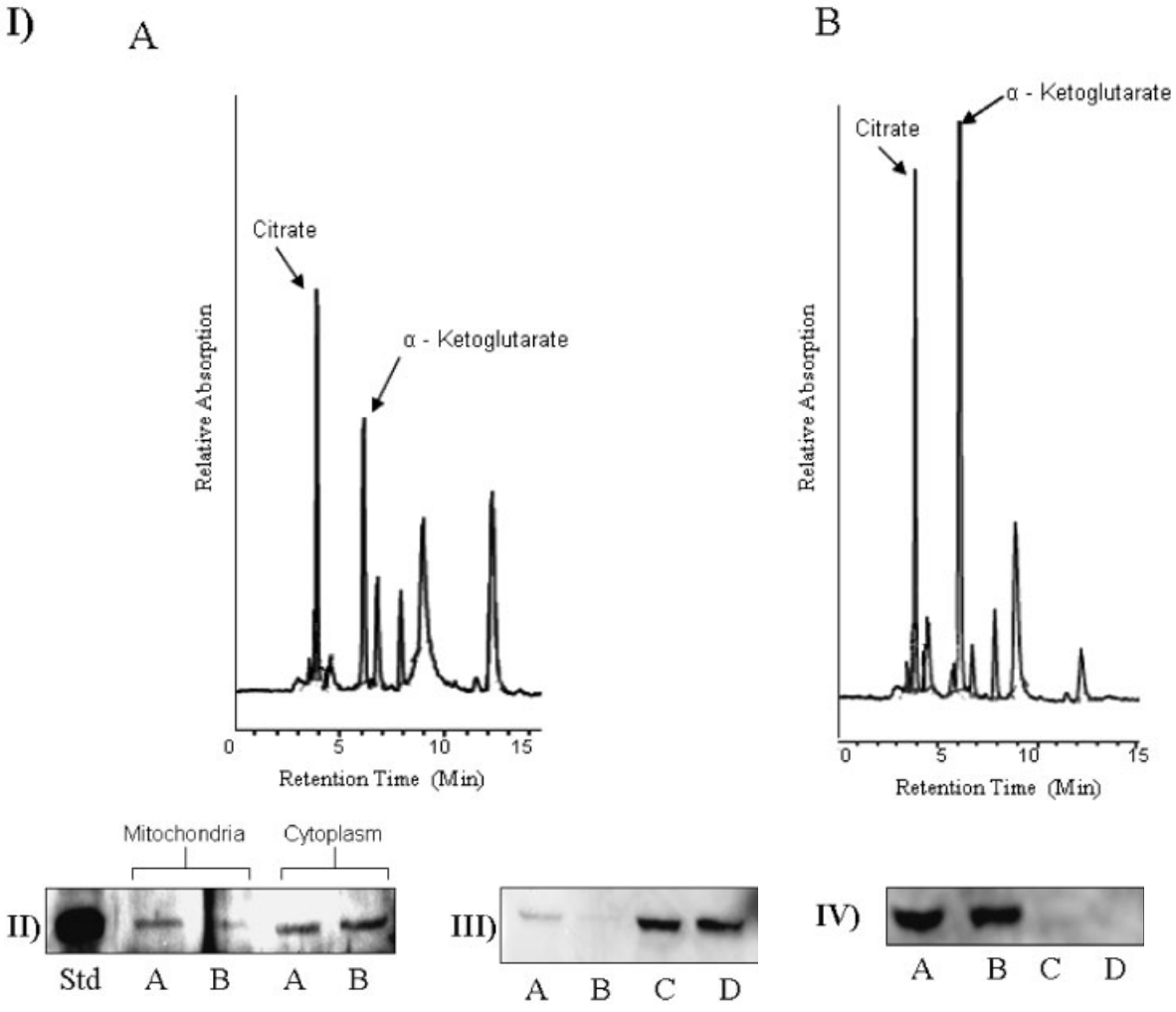

Figure 2. (I) HPLC analysis of citrate metabolism in HepG2 cells. Mitochondria were incubated for 1 h at 37 °C and then analysed. (A) Citrate cultures. (B) Zn-citrate cultures. (II) Immunoblot analysis of ACN in HepG2 cells exposed to citrate and Zn-citrate cultures. (A) Citrate stressed cells. (B) Zn-citrate stressed cells. Std corresponds to an ACN (porcine heart) purchased from Sigma. (III, IV) The purity of cellular fractions and equal loading were ascertained by immunoblot assays. (A) Cytoplasm from citrate culture. (B) Cytoplasm from Zn-citrate culture. (C) Mitochondrial fraction from citrate culture. (D) Mitochondrial fraction from Zn-citrate culture. (III) Immunoblot for VDAC. (IV) Immunoblot for F-Actin

that were treated with Zn and H_2O_2, respectively (Fig. 4, III and IV). As the activity and expression of several TCA cycle and ETC enzymes were perturbed by the presence of Zn, the ability of the mitochondria to produce ATP was assessed by HPLC. Incubation of control and Zn-stressed mitochondria in the presence of 1 mM citrate and 0.5 mM ADP revealed diminished ATP production in the Zn-stressed HepG2 cells. While control cells had a prominent ATP signal at 6.5 min, the signal at 6 min attributable to ADP, was more pronounced in the Zn-stressed cells (Fig. 5). Thus, indicating the diminished ability of the Zn-challenged cells to consume ADP and produce ATP.

The data in this report point to the negative impact of Zn on mitochondrial ATP production. Zn imposed an oxidative stress, severely impeding various TCA cycle enzymes and limiting energy production via oxidative phosphorylation. Toxic levels of Zn have been implicated in promoting oxidative stress, however; the molecular mechanism underlying this process is still unclear. In this study a marked reduction of the mitochondrial membrane potential in HepG2 cells challenged with Zn was observed. It is therefore not unlikely that this transition element may interfere with the mitochondrial enzymes involved in the generation of the proton gradient. Indeed, this soft acid metal can form strong interactions with enzymatic imidazole and sulphydryl groups. Numerous enzymes involved in the aerobic production of ATP contain active sites rich in these side chains (Quig, 1998). Although these interactions form the basis of the structural and functional role of zinc in biology, higher levels may impede the action of enzymes which rely on

DOI: 10.1002/jat

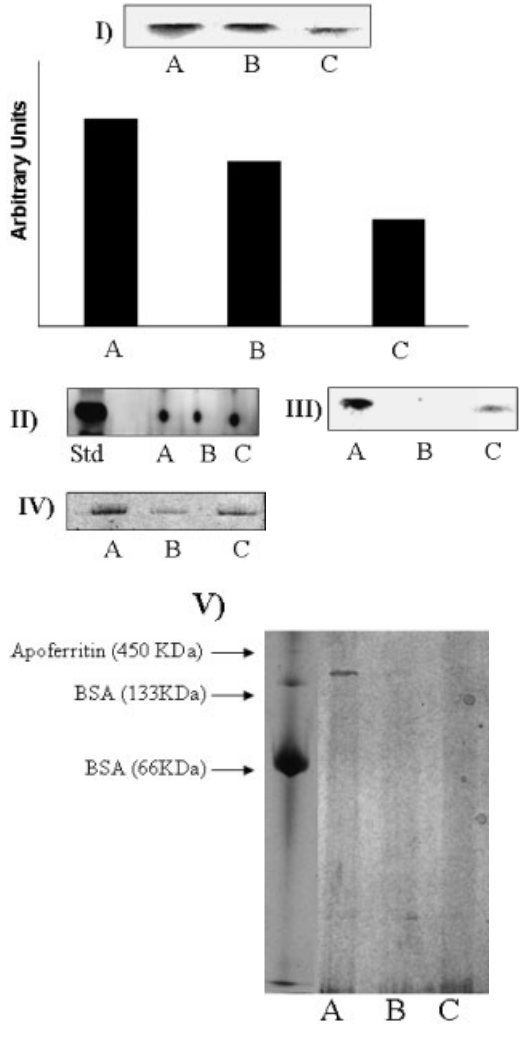

Figure 3. Activity and expression of α-KGDH. (A) Mitochondrial fraction isolated from citrate exposed cells. (B) Mitochondrial fraction isolated from Zn-citrate exposed cells. (C) Mitochondrial fraction isolated from H_2O_2 exposed cells. (I) In gel detection of α-KGDH activity. Bands were quantified using Scion Imaging for Windows. (II) 2D SDS-PAGE of α-KGDH; BN-PAGE activity bands followed by immunoblot analysis. Std corresponds to an α-KGDH (Porcine heart) purchased from Sigma. (III) In gel detection of NAD^+-ICDH in the cytoplasm. (IV, V) In gel activity staining for SDH and Cyt C Ox in mitochondria isolated from (A) citrate culture, (B) H_2O_2 and citrate culture, (C) Zn-citrate culture, (IV) SDH, (V) Cyt C Ox

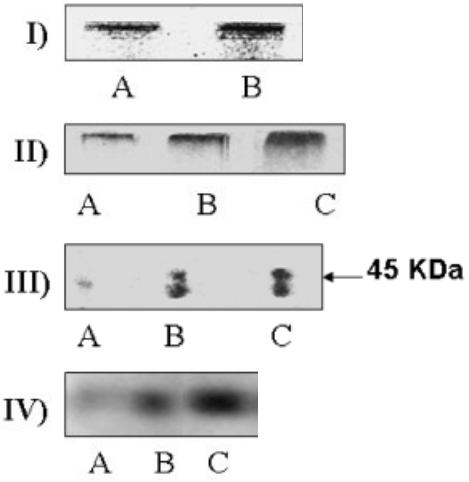

Figure 4. Activity stain and immunoblot analysis of ICDH in HepG2 cells exposed to (A) citrate, (B) Zn-citrate stress, (C) H_2O_2 and citrate stress. (I) In gel detection of $NADP^+$-ICDH in the cytoplasm. (II) In gel detection of $NADP^+$-ICDH in the mitochondria. (III) 2D SDS PAGE on $NADP^+$-ICDH in the mitochondria. (IV) 2D immunoblot of $NADP^+$-ICDH in the mitochondria

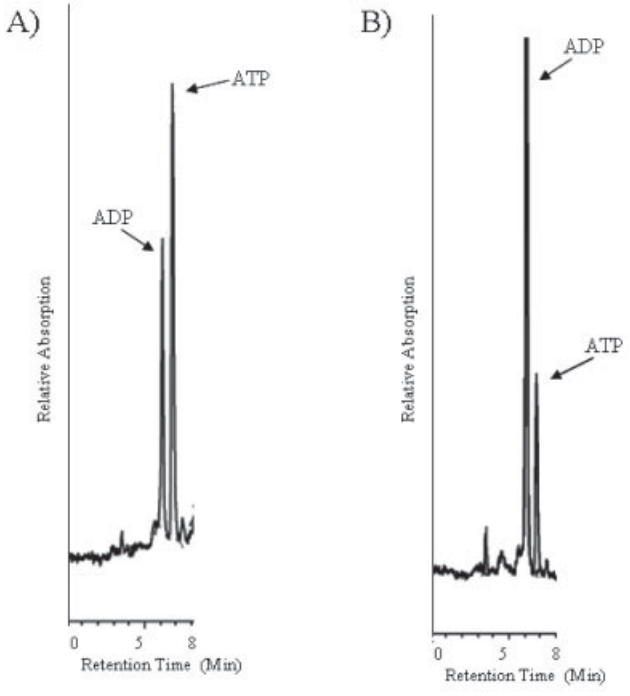

Figure 5. HPLC chromatographs displaying relative ATP and ADP levels in citrate and Zn-citrate stressed HepG2 cells. Mitochondria were incubated for 1 h at 37 °C. (A) Citrate culture. (B) Zn-citrate culture. ATP was monitored at 254 nm

catalytic thiols. The mitochondrial ACN seemed to be a potent target of Zn toxicity. The disruption of the expression of this enzyme may be due to the ability of Zn to perturb the Fe-S cluster necessary for catalysis. The proper functioning of mitochondrial ACN is critical to the commitment of citrate to anaplerosis and ATP production. The chromatographic data revealed the inability of Zn-stressed HepG2 mitochondria to metabolize this tricarboxylic acid effectively. A much higher signal confirmed the diminished capacity of ACN to isomerize citrate to isocitrate. Interestingly Zn did not hamper the expression of the cytoplasmic ACN enzyme. This observation is consistent with the role of the cytoplasmic ACN in initiating transcriptional events (Crichton *et al*., 2002;

DOI: 10.1002/jat

Mailloux *et al*., 2006a). Zn-mediated disruption of Fe-S dependent enzymes was not limited to ACN. Fe-S cluster-dependent enzymes such as SDH and Cyt C Ox also succumbed to the toxicity of Zn. The diminished activity of these enzymes would negate the production of mitochondrial ATP. The inability to produce ATP via O_2-dependent metabolism would have dire consequences, as this nucleotide is required to drive cellular processes. Indeed, HPLC analysis pointed to a decrease in ATP production in Zn-stressed mitochondria. These data are consistent with the lowered mitochondrial membrane potential as revealed by fluorescence microscopic assays (Jiang *et al*., 2001). In addition the H_2O_2-stressed HepG2 cells were also characterized with the lowered activity of the two oxidative phosphorylation enzymes. Metal-mediated disruption of Fe-S cluster dependent TCA cycle enzymes has been shown previously (Mailloux *et al*., 2006a; Middaugh *et al*., 2005). In fact, it has recently been shown that the bioavailability of Zn is tightly regulated within the intracellular environment. Small increments in Zn levels leads to the activation of a hypersensitive transcriptional switch ZntR, which modulates the availability of Zn in the femtomolar range (Changela *et al*., 2003; Outten and O'Halloran, 2001). The tight regulation of intracellular Zn levels may be due to its affinity for biological active sites. Indeed this divalent cation has been implicated in oxidative stress and numerous pathologies (Barceloux, 1999; Fosmire, 1990; Koh *et al*., 1996). Competition for Fe-S binding sites may displace free Fe and contribute to oxidative tension within the cell. This divalent cation has also been reported to interact with thiol groups of antioxidants such as glutathione (Nappi and Vass, 1997; Sipos *et al*., 2002). This would inevitably lead to the depletion of reduced glutathione in the intracellular environment thus contributing to oxidative tension. In addition Zn-mediated inhibition of SDH and Cyt C Ox would certainly contribute to e^- leakage and ROS production in the mitochondria. Mitochondrial activity generates a highly oxidative environment as it is the site of oxidative phosphorylation (Martin *et al*., 1996; Shigenaga *et al*., 1994). In this study two critical NAD^+-dependent decarboxylating enzymes of the TCA cycle, ICDH and KGDH, exhibited lower activity and expression within the Zn-stressed mitochondria. Interestingly, no reduction in expression of KGDH was observed, even though the activity was considerably less. This observation may be attributable to the redox sensitive lipoic acid residue on the E_2-subunit of this enzyme. Zn may interact with the available thiols on the enzyme rendering it inactive. In addition, an oxidative environment may promote the oxidation of the thiols. The inhibition of these two decarboxylation enzymes was also evident in the presence of H_2O_2. Hence, it is tempting to postulate that the reduction in activity of this enzyme without a concomitant diminution in expression may contribute to the reduction of the oxidative tension. ROS production during metal toxicity is a well documented phenomenon. NADPH-dependent enzymes such as cytoplasmic ICDH, malic enzyme and glucose-6-phosphate dehydrogenase have recently been identified as key contributors to the antioxidant system (Beriault *et al*., 2007). In the Zn-stressed HepG2 cells, the cytoplasmic $NADP^+$-ICDH had much higher activity. Mitochondrial $NADP^+$-ICDH also displayed higher activity in the Zn treated cells. These observations point to an attempt by the cell to cope with oxidative stress by producing large amounts of NADPH. NADPH is crucial in providing the cells with the reducing power necessary to regenerate antioxidants such as catalase, SOD and glutathione (Arivazhagan *et al*., 2000; Fang *et al*., 2002). Thus, the enhanced production of NADPH would ensure the maintenance of the reducing environment necessary for scavenging ROS. This observation may also account for the accumulation of α-KG. α-KG is known as a powerful antioxidant and utilized in the prevention of inflammation during surgery (Kjellman *et al*., 1995; Velvizhi *et al*., 2002). This metabolite has been shown to accumulate as a consequence of metal toxicity (Zatta *et al*., 2000). The accumulation of α-KG observed in this instance may be due to the inhibition of KGDH by Zn and an overactive mitochondrial $NADP^+$-ICDH. Hence, this α-keto acid may serve as an important tool against oxidative stress. The modulation of these TCA cycle enzymes would serve as a natural antioxidant defense system which would aid in attenuating oxidative stress. Therefore, it is not unlikely that the TCA cycle can serve to regulate the oxidative milieu within the mitochondria by modulating key enzymes. The oxidation and reduction of the lipoic acid residue on the E_2-subunit may serve such a function.

In conclusion, this study demonstrates that Zn exerts its toxic influence by creating an oxidative environment and interfering with several critical enzymes that participate in the TCA cycle and ETC. This inhibition severely restricts the ability of the cell to generate ATP, an ingredient essential for the proliferation and survival of the cell. This is the first demonstration of the upregulation of the mitochondrial $NADP^+$-ICDH as a consequence of oxidative stress induced by Zn toxicity. Thus it is quite likely that an ineffective TCA cycle and oxidative phosphorylation may be important contributing factors in various Zn-triggered pathologies.

Acknowledgements—This work was supported by funding from Industry Canada.

References

Abordo EA, Minhas HS, Thornalley PJ. 1999. Accumulation of alpha-oxoaldehydes during oxidative stress: a role in cytotoxicity. *Biochem. Pharmacol.* **58**: 641–648.

Arivazhagan P, Thilakavathy T, Panneerselvam C. 2000. Antioxidant lipoate and tissue antioxidants in aged rats. *J. Nutr. Biochem.* **11**: 122–127.

Aydin S, Yargicoglu P, Derin N, Aliciguzel Y, Abidin I, Agar A. 2005. The effect of chronic restraint stress and sulfite on visual evoked potentials (VEPs): relation to lipid peroxidation. *Food Chem. Toxicol.* **43**: 1093–1101.

Barceloux DG. 1999. Zinc. *J. Toxicol. Clin. Toxicol.* **37**: 279–292.

Beriault R, Hamel R, Chenier D, Mailloux RJ, Joly H, Appanna VD. 2007. The overexpression of NADPH-producing enzymes counters the oxidative stress evoked by gallium, an iron mimetic. *Biometals* **20**: 165–176.

Bradford MM. 1976. A rapid and sensitive method for the quantitation of microgram quantities of protein utilizing the principle of protein-dye binding. *Anal. Biochem.* **72**: 248–254.

Canzoniero LM, Turetsky DM, Choi DW. 1999. Measurement of intracellular free zinc concentrations accompanying zinc-induced neuronal death. *J. Neurosci.* **19**: RC31.

Changela A, Chen K, Xue Y, Holschen J, Outten CE, O'Halloran TV, Mondragon A. 2003. Molecular basis of metal-ion selectivity and zeptomolar sensitivity by CueR. *Science* **301**: 1383–1387.

Coleman JE. 1992. Zinc proteins: enzymes, storage proteins, transcription factors, and replication proteins. *Annu. Rev. Biochem.* **61**: 897–946.

Costello LC, Liu Y, Franklin RB, Kennedy MC. 1997. Zinc inhibition of mitochondrial aconitase and its importance in citrate metabolism of prostate epithelial cells. *J. Biol. Chem.* **272**: 28875–28881.

Crichton RR, Wilmet S, Legssyer R, Ward RJ. 2002. Molecular and cellular mechanisms of iron homeostasis and toxicity in mammalian cells. *J. Inorg. Biochem.* **91**: 9–18.

Dinely KE, Votyakova TV, Reynolds IJ. 2003. Zinc inhibition of cellular energy production: implication for mitochondria and neurodegeneration. *J. Neurochem.* **85**: 563–570.

Dumont A, Hehner SP, Hofmann TG, Ueffing M, Droge W, Schmitz ML. 1999. Hydrogen peroxide-induced apoptosis is CD95-independent, requires the release of mitochondria-derived reactive oxygen species and the activation of NF-kappaB. *Oncogene* **18**: 747–757.

Fang YZ, Yang S, Wu G. 2002. Free radicals, antioxidants, and nutrition. *Nutrition* **18**: 872–879.

Fernie AR, Carrari F, Sweetlove LJ. 2004. Respiratory metabolism: glycolysis, the TCA cycle and mitochondrial electron transport. *Curr. Opin. Plant Biol.* **7**: 254–261.

Fosmire GJ. 1990. Zinc toxicity. *Am. J. Clin. Nutr.* **51**: 225–227.

Gazaryan IG, Krasnikov BF, Ashby GA, Thorneley RN, Kristal BS, Brown AM. 2002. Zinc is a potent inhibitor of thiol oxidoreductase activity and stimulates reactive oxygen species production by lipoamide dehydrogenase. *J. Biol. Chem.* **277**: 10064–10072.

Hambidge M. 2000. Human zinc deficiency. *J. Nutr.* **130**: 1344S–1349S.

Jiang D, Sullivan PG, Sensi SL, Steward O, Weiss JH. 2001. Zn(2+) induces permeability transition pore opening and release of pro-apoptotic peptides from neuronal mitochondria. *J. Biol. Chem.* **276**: 47524–47529.

Kjellman U, Bjork K, Ekroth R, Karlsson H, Jagenburg R, Nilsson F, Svensson G, Wernerman J. 1995. Alpha-ketoglutarate for myocardial protection in heart surgery. *Lancet* **345**: 552–553.

Koh JY, Suh SW, Gwag BJ, He YY, Hsu CY, Choi DW. 1996. The role of zinc in selective neuronal death after transient global cerebral ischemia. *Science* **272**: 1013–1016.

Laemmli UK. 1970. Cleavage of structural proteins during the assembly of the head of bacteriophage T4. *Nature* **227**: 680–685.

Mailloux RJ, Appanna VD. 2007. Aluminum toxicity triggers the nuclear translocation of HIF-1alpha and promotes anaerobiosis in hepatocytes. *Toxicol. In Vitro* **21**: 16–24.

Mailloux RJ, Hamel R, Appanna VD. 2006a. Aluminum toxicity elicits a dysfunctional TCA cycle and succinate accumulation in hepatocytes. *J. Biochem. Mol. Toxicol.* **20**: 198–208.

Mailloux RJ, Singh R, Appanna VD. 2006b. In-gel activity staining of oxidized nicotinamide adenine dinucleotide kinase by blue native polyacrylamide gel electrophoresis. *Anal. Biochem.* **359**: 210–215.

Manev H, Kharlamov E, Uz T, Mason RP, Cagnoli CM. 1997. Characterization of zinc-induced neuronal death in primary cultures of rat cerebellar granule cells. *Exp. Neurol.* **146**: 171–178.

Martin GM, Austad SN, Johnson TE. 1996. Genetic analysis of ageing: role of oxidative damage and environmental stresses. *Nat. Genet.* **13**: 25–34.

Middaugh J, Hamel R, Jean-Baptiste G, Beriault R, Chenier D, Appanna VD. 2005. Aluminum triggers decreased aconitase activity via Fe-S cluster disruption and the overexpression of isocitrate dehydrogenase and isocitrate lyase: a metabolic network mediating cellular survival. *J. Biol. Chem.* **280**: 3159–3165.

Nappi AJ, Vass E. 1997. Comparative studies of enhanced iron-mediated production of hydroxyl radical by glutathione, cysteine, ascorbic acid, and selected catechols. *Biochim. Biophys. Acta* **1336**: 295–302.

Outten CE, O'Halloran TV. 2001. Femtomolar sensitivity of metalloregulatory proteins controlling zinc homeostasis. *Science* **292**: 2488–2492.

Piao F, Yokoyama K, Ma N, Yamauchi T. 2003. Subacute toxic effects of zinc on various tissues and organs of rats. *Toxicol. Lett.* **145**: 28–35.

Prasad AS. 1996. Zinc deficiency in women, infants and children. *J. Am. Coll. Nutr.* **15**: 113–120.

Quig D. 1998. Cysteine metabolism and metal toxicity. *Altern. Med. Rev.* **3**: 262–270.

Religa D, Strozyk D, Cherny RA, Volitakis I, Haroutunian V, Winblad B, Naslund J, Bush AI. 2006. Elevated cortical zinc in Alzheimer disease. *Neurology* **67**: 69–75.

Samizo K, Ishikawa R, Nakamura A, Kohama K. 2001. A highly sensitive method for measurement of myosin ATPase activity by reversed-phase high-performance liquid chromatography. *Anal. Biochem.* **293**: 212–215.

Sandstead HH. 1991. Zinc deficiency. A public health problem? *Am. J. Dis. Child.* **145**: 853–859.

Schagger H, von Jagow G. 1991. Blue native electrophoresis for isolation of membrane protein complexes in enzymatically active form. *Anal. Biochem.* **199**: 223–231.

Sensi SL, Yin HZ, Weiss JH. 1999. Glutamate triggers preferential Zn2+ flux through Ca2+ permeable AMPA channels and consequent ROS production. *Neuroreport* **10**: 1723–1727.

Shannon JE. 1978. Tissue culture viability assays — a review of the literature. *Cryobiology* **15**: 239–241.

Shigenaga MK, Hagen TM, Ames BN. 1994. Oxidative damage and mitochondrial decay in aging. *Proc. Natl Acad. Sci. USA* **91**: 10771–10778.

Sipos K, Lange H, Fekete Z, Ullmann P, Lill R, Kispal G. 2002. Maturation of cytosolic iron-sulfur proteins requires glutathione. *J. Biol. Chem.* **277**: 26944–26949.

Steinebach OM, Wolterbeek HT. 1993. Effects of zinc on rat hepatoma HTC cells and primary cultured rat hepatocytes. *Toxicol. Appl. Pharmacol.* **118**: 245–254.

Takeda A, Minami A, Takefuta S, Tochigi M, Oku N. 2001. Zinc homeostasis in the brain of adult rats fed zinc-deficient diet. *J. Neurosci. Res.* **63**: 447–452.

Velvizhi S, Dakshayani KB, Subramanian P. 2002. Protective influences of alpha-ketoglutarate on lipid peroxidation and antioxidant status in ammonium acetate treated rats. *Indian J. Exp. Biol.* **40**: 1183–1186.

Walsh CT, Sandstead HH, Prasad AS, Newberne PM, Fraker PJ. 1994. Zinc: health effects and research priorities for the 1990s. *Environ. Health Perspect.* **102** (Suppl 2): 5–46.

Zatta P, Lain E, Cagnolini C. 2000. Effects of aluminum on activity of Krebs cycle enzymes and glutamate dehydrogenase in rat brain homogenate. *Eur. J. Biochem.* **267**: 3049–3055.

DOI: 10.1002/jat